1996 National Heat Transfer Conference
Instrumentation and Measurements Symposium
August 3-6, 1996, Houston, TX SAND96-XXXXC

# PRESSURE EFFECTS ON BUBBLE-COLUMN FLOW CHARACTERISTICS



D. R. Adkins, K. A. Shollenberger, T. J. O'Hern, and J. R. Torczynski
Engineering Sciences Center
Sandia National Laboratories
Albuquerque, NM 87185

## ABSTRACT

Bubble-column reactors are used in the chemical processing industry for two-phase and three-phase chemical reactions. Hydrodynamic effects must be considered when attempting to scale these reactors to sizes of industrial interest, and diagnostics are needed to acquire data for the validation of multiphase scaling predictions. This paper discusses the use of differential pressure (DP) and gamma-densitometry tomography (GDT) measurements to ascertain the gas distribution in a two-phase bubble column reactor. Tests were performed on an industrial scale reactor (3-m tall, 0.48-m inside diameter) using a 5-Curie cesium-137 source with a sodium-iodide scintillation detector. GDT results provide information on the time-averaged cross-sectional distribution of gas in the liquid, and DP measurements provide information on the time and volume averaged axial distribution of gas. Close agreement was observed between the two methods of measuring the gas distribution in the bubble column. The results clearly show that, for a fixed volumetric flowrate through the reactor, increasing the system pressure leads to an increase in the gas volume fraction or "gas holdup" in the liquid. It is also shown from this work that GDT can provide useful diagnostic information on industrial scale bubble-column reactors.

## NOMENCLATURE

$a_0$ = constant term of $\psi(r,R)$ curve fit (nondimensional)
$a_1$ = quadratic term of $\psi(r,R)$ curve fit (nondimensional)
$b_0$ = constant term of $\psi(x,R)$ curve fit (nondimensional)
$b_1$ = quadratic term of $\psi(x,R)$ curve fit (nondimensional)
$g$ = gravitational acceleration (m/s$^2$)
$u_g$ = superficial gas velocity (m/s)
$r$ = radial location (m)
$u_l$ = superficial liquid velocity (m/s)
$x$ = cross-section location of gamma trace (m)
$z$ = axial location (m)
$D$ = column inner diameter, $D = 2R$ (m)
$I$ = gamma intensity (photons/s)
$I_o$ = incident intensity (photons/s)

$L$ = length (m)
$N$ = gamma photon count (nondimensional)
$P$ = pressure (Pa)
$R$ = column inner radius (m)
$\Delta\rho$ = liquid minus gas density ($kg/m^3$)
$\varepsilon_g$ = gas volume fraction ($m^3/m^3$)
$\mu$ = attenuation coefficient ($m^{-1}$)
$\psi$ = normalized attenuation coefficient (nondimensional)
$\rho$ = density ($kg/m^3$)
$\sigma$ = liquid surface tension (N/m)
$\tau$ = detector time constant (s)

## INTRODUCTION

Bubble-column reactors are used in the synthesis of many important chemical compounds. In the Fischer-Tropsch process, for example, a mixture of $H_2$ and $CO_2$ from coal gasification is bubbled up through a catalyst-laden liquid hydrocarbon for the production of liquid fuels. The distribution of gas and solids within the liquid has a major impact on the efficiency of the process. As gas flowrates are boosted to increase production, the bouancy-driven hydrodynamics can cause a poor spatial distribution of gas bubbles and lower conversion rates.

Most reactor systems are required to operate at high pressures, and the influence of the pressure on the hydrodynamics is of particular interest. In a study of bubble formation from a single orifice, LaNauze and Harris [1974] found that for a given gas flowrate, an increase in system pressure causes smaller, but more frequent, bubbles to be formed. They attribute this behavior to the increased contribution of the momentum of the gas to the bubble-formation process. Gas momentum imparts a greater upward force on the bubble at higher pressures and causes the bubble to depart from the orifice sooner. The increased frequency of bubble formation was found to cause more coalescence and interaction of the bubbles departing from the orifice. For a fixed volumetric gas flowrate (determined at the system pressure), the volume of individual bubbles decreased by at least a factor of two as the pressure increased from one to ten atmospheres. Above ten atmospheres, LaNauze and Harris observed that the bubble volume remained relatively constant with further pressure increases. They also found that increasing the flowrate at a fixed pressure caused the bubble volume to increase. At atmospheric pressure, the bubble volume increased linearly with gas flowrate, but as the system pressure increases, the volume of individual bubbles was increasingly less influenced by the gas flowrate. Theories that were developed by Davidson and Schuler [1960] and later extended by LaNauze and Harris demonstrated fairly good correlation with experimental results in these earlier works.

While studies on single-orifice systems provide some insights on the relationships between operating pressures, flowrates and bubble sizes, the bubble formation hydrodynamics become much more complicated in systems with multiple gas injection points (such as spargers). The crossflow of liquid that develops during bubble formation at

one orifice can influence the departure of bubbles at adjacent orifices. In addition, bubble induced pressure fluctuations in the gas plenum of the sparger are coupled to the formation and departure of bubbles. This paper is focused on studying the bulk hydrodynamics of the system rather than on the development and subsequent evolution of individual bubbles.

To understand the influence of operating and design parameters on the hydrodynamics of the bubble column, it is necessary to have diagnostic capabilities to measure the spatial distribution of gas in the bubble-column reactors. Gamma-densitometry tomography (GDT) is one method of measuring gas holdup (gas volume fraction) distributions in multiphase flows. Brown et al. [1993] and Reda et al. [1981] discuss applying GDT to liquid saturation of porous media, and Kumar et al. [1995] recently published an extensive review of GDT applied to multiphase flow systems. The basic premise of GDT is that gamma photons are attenuated by scattering and absorption as they pass through matter. The attenuation is a function only of the energy of the gamma photon and the attenuation coefficient, $\mu$, of the material. If the incident gamma beam has an intensity $I_o$ (in counts per second), then the intensity after passing through a material of length $L$ will be $I = I_o \exp(-\mu L)$. For a multiphase mixture, the attenuation coefficient is the sum of the products of the volume fractions of the phases with their attenuation coefficients. Thus, by measuring the ratio $I/I_o$, the average attenuation coefficient along path $L$ can be determined. A tomographic reconstruction of the attenuation coefficient, and therefore the phase distribution, can be made using information from multiple scans through the test object. Photon emission from the gamma source fluctuates as a Poisson process and the uncertainty in the intensity measurement is related to $(1/N)^{1/2}$ where $N$ is the number of photons. To obtain a count that is high enough to give meaningful results, the attenuation will by necessity be a time-averaged result along the path $L$. With this time-averaged attenuation coefficient, the gas distribution within the column of liquid can be determined.

## SYSTEM DESCRIPTION

The industrial-scale bubble column that was used in these experiments is shown in Figure 1. The stainless steel vessel is 3 m tall and has a 0.48-m inside diameter with a wall thickness of 1.27 cm. Instrumentation and view ports were placed in six axial locations 0.48 m apart. Differential pressure transducers were installed in each of these locations to measure pressures along the column. Air is injected into a liquid-filled column through a sparger located near the bottom of the vessel. The sparger is a 15-cm diameter ring formed from 1.1-cm ID stainless steel tubing. Twelve holes, 3.18 mm in diameter, are in the top surface of the sparger ring. To date, superficial gas velocities of up to 0.40 m/s have been produced in the system with a corresponding gas volume fraction or "gas holdup" of 40 %. The flowrate of the gas is measured with an orifice-plate flowmeter to an accuracy of 1.7 %.

A portable GDT system is used to measure the gas volume fraction within the column. Gamma photons from a 5-Curie cesium-137 source are collimated through a 6.35-mm ID tube, projected through the test object and onto a sodium-iodide

photomultiplier tube (PMT). The PMT gamma detector is located in a lead shield with a 6.36-mm ID collimating tube that photons must pass through to reach the detector. The source and the detector are mounted on a heavy duty traverse system that can translate 60 cm vertically (along the axis of the column) and 60 cm horizontally. Both the step size and the dwell time of the traverse system can be selected to facilitate data acquisition.

Signals from the PMT pass through a preamplier and are then relayed to a spectrum amplifier. The spectrum amplifier generates a pulse with a peak that is proportional to energy of each photon the PMT detects. The output from the spectrum amplifier goes to a single channel analyzer (SCA) that selects a narrow window of pulse amplitude centered about the 661.6 keV cesium-137 energy peak. It is possible with the system to count pulses from the SCA over a selected time period or, alternatively, to measure the time required for a selected number of pulses to be counted. This last alternative was chosen for the current series of tests, so the number of detected counts remains constant for each source/detector location. The GDT system is also equipped with a multichannel analyzer that measures the count rate for a series of differential energy bands across the energy spectrum. For the series of tests reported here, the multichannel analyzer was used to calibrate the window settings on the SCA.

In addition to the GDT system, the column was also equipped with differential pressure transducers at the six instrumentation ports along the length of the bubble column. Variable reluctance differential pressure transducers manufactured by Validyne (Model DP15) were selected for this application. A pickup coil in the Validyne transducer measures the displacement of a diaphragm to determine the pressure. Diaphragms are selected for the desired pressure range. One side of each differential pressure transducer was connected to an instrumentation port along the column, and the other side was plumbed through a manifold to the air space at the top of the bubble column. The gauge pressure at the top and upstream of the column were also measured with Validyne differential pressure transducers. Differential pressure transducers along the column had a maximum span of 34 kPa (5 psi) with an accuracy of 0.65 kPa. The gauge pressure at the top of the column had a maximum span of 552 kPa (80 psi) with an accuracy of $\pm 0.25\%$ of full scale.

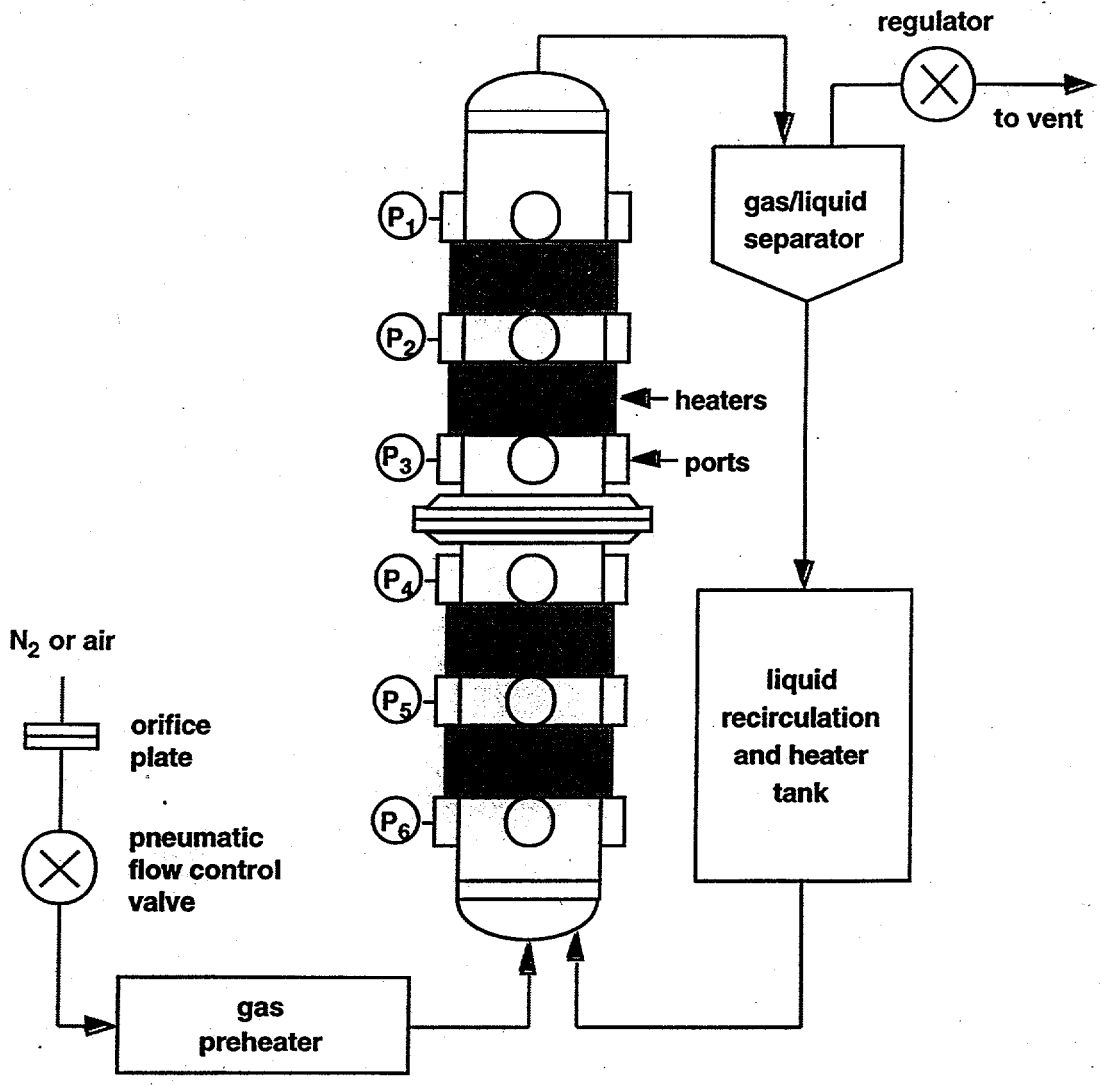


Figure 1. Configuration of the industrial-scale bubble column reactor. The column is 3 m tall and has a 0.48-m ID.

## RECONSTRUCTION TECHNIQUES

Tomographic reconstruction techniques are discussed in detail elsewhere [Herman, 1983, and Howard, 1985], and a more in-depth description of the algorithm used for our system is provided by Torczynski et al. [1996]. For the work presented here, it was assumed that the time-averaged flow in the column is axisymmetric. This assumption appears to be reasonable since the attenuation data from horizontal scans across the column were found to be relatively symmetric. Figure 2 shows the measured intensity (or gamma count rate) as a function of horizontal location for a fixed axial (vertical) location along the column. Results shown are for three cases; (1) an air-filled column, (2) a water-filled column, and (3) a water-filled column with a superficial gas velocity of 0.086 m/s. When the tank is empty, the count rate is high enough that the system is unable to count all of the gamma photons intercepted by the detector. The true count rate is estimated using the correlation

$$I_{true} = \frac{I_{measured}}{1 - \tau I_{measured}} ,$$

where $\tau$ is the time constant inherent to the detector and the counting electronics [Knoll, 1979]. The time constant was estimated by measuring count rates for a set of rectangular calibration water tanks of known length and then inverting the data to solve for a value of $\tau$ that gave the best fit. It was found that $\tau$ was on the order of 10 μs (or less), but the correction made little difference in the final estimate of the gas volume fraction. The correction would be much more important for a thinner-walled vessel where count rates are higher.

Tomographic reconstruction entails transforming the beam attenuation data along lines intersecting the column into a measure of the radial distribution of the attenuation corresponding to the time-averaged gas distribution. The first step in the tomographic reconstruction to determine the radial gas distribution in the bubble column is to normalize the attenuation data by the difference in the attenuation of the full and empty tanks. The normalized attenuation, $\psi_i$, at each position, $x_i$, is defined as

$$\psi_i = \frac{\ln\left(I_i^{empty}\right) - \ln\left(I_i^{flow}\right)}{\ln\left(I_i^{empty}\right) - \ln\left(I_i^{full}\right)} .$$

Figure 3 shows the normalized attenuation coefficient for the data provided in Figure 2. Since the average gas volume distribution is assumed to be axisymmetric, it is possible to represent the attenuation data with an even powered polynomial. A fit of the data set $\{(x_i, \psi_i)\}$ is performed to form a function $\psi(x,R) = b_0 + b_1(x/R)^2$. Coefficients $b_0$ and $b_1$ are then used to determine the coefficients $a_0$ and $a_1$ of the corresponding radial variation of the normalized attenuation coefficient, $\psi(r,R) = a_0 + a_1(r/R)^2$ . The Abel transform is used to determine the relationship between the polynomial coefficients of the functions $\psi(x,R)$ and $\psi(r,R)$ within the domain of $R$. Torczynski et al. [1996] provide a generalized expression of this transform for higher order polynomials. For a quadratic fit, however, the

transformation simplifies to $a_0 = b_0 - b_1/2$ and $a_1 = 3b_1/2$. The normalized attenuation coefficient $\psi(r,R)$ ranges from zero for an empty tank to a value of one for a full tank. In a two-phase system, $\psi(r,R)$ corresponds to the liquid volume fraction in the column. Figure 3 shows the quadratic fit of the attenuation coefficient along with the reconstructed prediction of the liquid volume fraction. The radial gas volume fraction distribution, $\varepsilon_g(r,R)$, is simply $1-\psi(r,R)$.

The GDT results provide measurement of the time averaged gas volume distribution in horizontal slices of the bubble column. To complement these results, the pressure measurements can yield a measurement of the volume averaged gas volume fraction along the length of the column. If shear forces along the walls of the column are neglected, then the pressure gradient along the column is hydrostatic and given by the expression

$$\frac{dP}{dz} = -\rho_{mix}\, g \approx -\left(1-\varepsilon_g\right)\rho_{liquid} g\,,$$

where the sign, of course, indicates that the pressure decreases up the column. Pressure measurements at discrete locations can be used to obtain an estimate of $dP/dz$, and the result can then be used to determine the average gas volume fraction for the section.

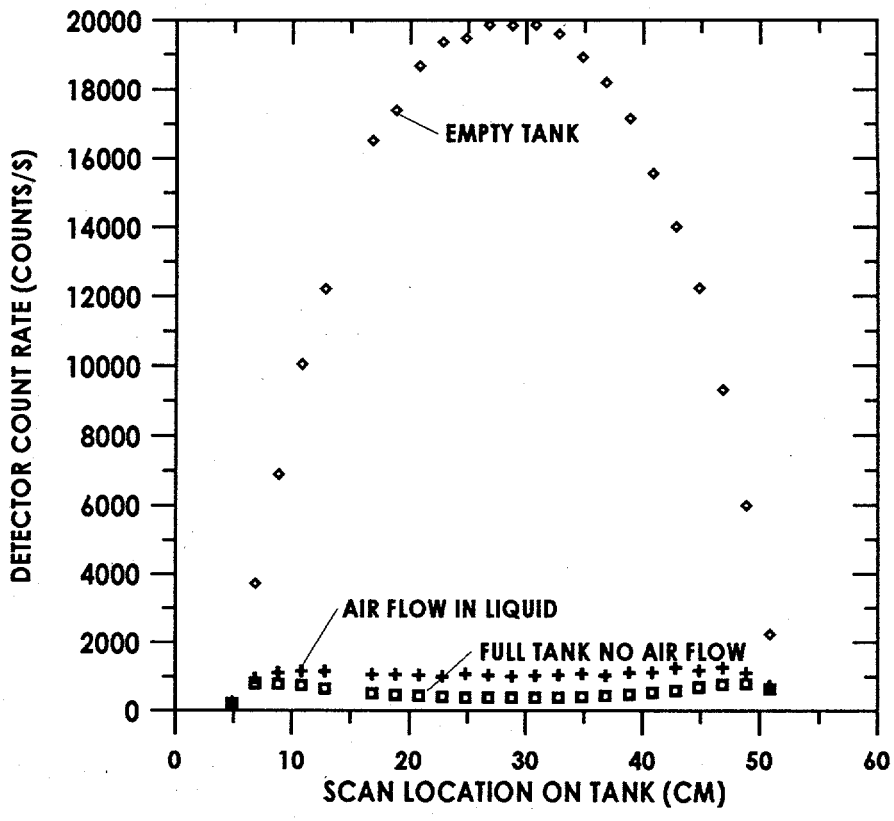


Figure 2. Gamma count rate vs. location for full and empty tank, and tank with air flow. Measurements were made along a horizontal path at an axial location two diameters (1 m) above the sparger.

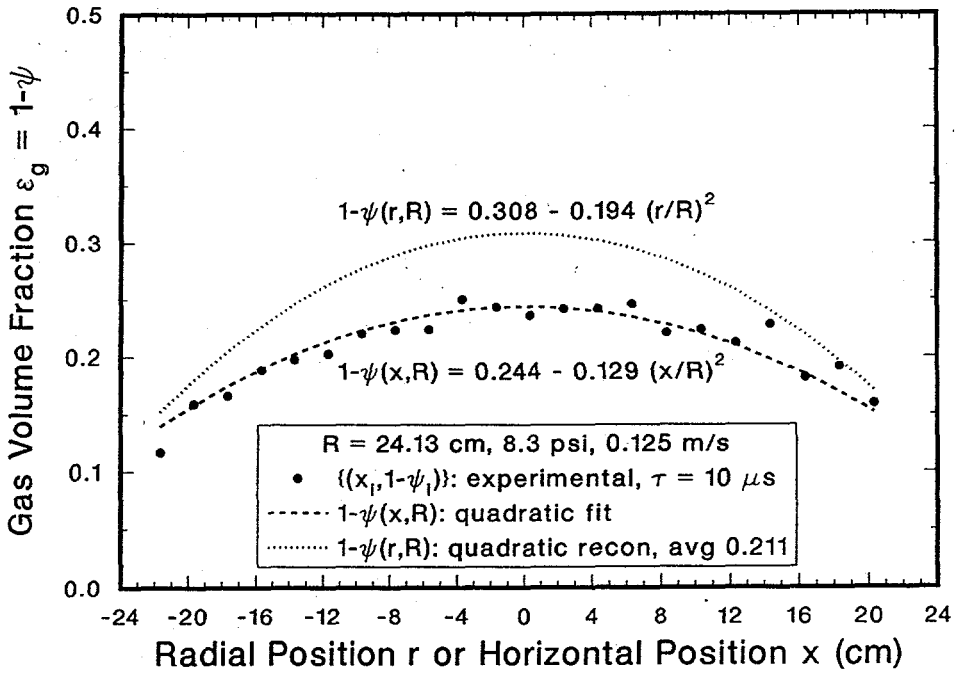


Figure 3. Reconstructed average gas distribution for an assumed axisymmetric profile.

## RESULTS

The bubble column was filled with water to give an effective *L/D* of 4 (as measured from the top of the sparger). Air was injected into the tank at superficial velocities ranging up to 0.16 m/s, and the gas flow at the top of the column was regulated to pressurize the tank. A large pressure drop in the exhaust line leaving the tank often dominated the discharge pressure and limited the minimum operating pressure of the system. The system pressure referred to in the following discussion is the pressure at the top of the tank in the gas-filled head space.

Figure 4 shows the gas holdup along the length of the bubble column based on differential pressure measurements. The reported gas holdup represents a volume averaged gas volume fraction for each of the five regions between the pressure transducers. Pressure data was collected at 100 Hz and then averaged over 25 seconds to obtain the pressure used in the gas holdup calculations. Measurements in the lower three

regions show that, as the superficial gas velocity increases, the holdup increases, as expected. There is no clear explanation for the somewhat lower gas holdup near the middle of the tank. The relatively high gas volume fractions in the top two regions indicate that pressure transducers at 4.6 and 5.5 m are in air during most of the data averaging time. At higher gas velocities, liquid is lofted higher into the column, and the pressure transducers at 4.6 and 5.5 m become submerged. Based on these measurements, the top two regions of the bubble column contain a frothy mixture with about a 40% gas volume fraction when the superficial gas velocity exceeds about 0.13 m/s.

Results in Figure 4, which were taken at a headspace pressure of 165 kPa (24 psig), can be compared with the results in Figure 5 for a 345 kPa (50 psig) headspace pressure. In general, the results are similar, but a careful examination shows that the gas holdup does increase with pressure for a given superficial velocity. Zuber and Findlay [1965] found that for churn-turbulent flows, the gas volume fraction can be correlated to the superficial velocity through the expression

$$\frac{u_g}{\varepsilon_g} = C_0\left(u_g + u_l\right) + 1.53\left(\sigma g \Delta\rho / \rho_l^2\right)^{0.25},$$

where $u_g$ is the superficial gas velocity and $u_l$ is the superficial liquid velocity which equals zero when the bubble column is in steady operation. The term $u_g/\varepsilon_g$ is actually the interstitial velocity of the bubbles traveling through the liquid, and the last term of the right-hand side of this equation is an empirical expression for the terminal rise velocity of bubbles in churn-turbulent flow [Cheremisinoff and Gupta, 1983]. The factor $C_0$ is a function of the operating pressure of the system.

Figure 6 shows the measured gas holdup in the bubble column as a function of superficial gas velocity at pressures ranging from about 2 to 4 atmospheres. Results from Zuber and Findlay's model are also shown Figure 6 ($C_0$ was chosen to give the best fit to the data). Gas holdup estimates were based on the differential pressure measurements made in the three lower regions of the column. The increase in gas holdup with pressure at any given superficial gas velocity indicates that the interstitial velocity of the bubbles decreases with pressure. The data correlate well with Zuber and Findlay's model which is shown as solid lines in Figure 6. The general decline of $C_0$ with pressure implies that the superficial velocity has a decreasing influence on the interstitial velocity as the system pressure increases.

The observation that the interstitial velocity decreases with pressure coincides with LaNauze and Harris's [1974] finding that, for a fixed gas flowrate, the bubble size decreases with system pressure. Bouyancy forces scale with the cube of the bubble diameter, and drag forces on the bubble scale with the square of the diameter. By balancing forces on the bubble, it follows that the interstitial velocity scales with the bubble diameter. The decrease in the interstitial velocity with an increase in pressure therefore implies that the bubble size also has decreased with an increase in pressure.

The radial distribution of the gas volume fraction at a location 0.96 m ($L/D = 2$) above the sparger is shown in Figure 7 for several operating pressures and superficial gas

velocities. Gamma attenuation measurements were made at 2-cm intervals across the column to provide data for these GDT reconstructions. 20,000 gamma photon counts were detected at each position before the system traversed to the next location, so the data collection time for a scan was approximately 10 minutes. Since the pressure and the superficial gas velocity cannot be independently controlled at this time, it is difficult to make generalizations about the impact of these parameters separately on the gas distribution in the bubble column. At the highest measured gas flowrate and lower pressures, the GDT reconstructions show that the gas volume fraction was about a factor of two higher in the middle than near the edges of the bubble column. The profile of the gas volume fraction becomes flatter as the superficial gas velocity decreases and the pressure increases. With a more controlled test in the near future, the independent influence of the system pressure and gas velocity will be examined.

A comparison between the average gas volume fraction at a cross section based on GDT, and the volume averaged gas volume fraction based on differential pressure measurements is given in Table 1. Pressure results were based on measurements from transducers on either side of the GDT scan. The agreement between the two methods of estimating gas holdup is quite good as the data show.

| System pressure, kPa (psig) | Superficial gas velocity, m/s | Gas holdup measured with GDT, % | Gas holdup measured with DP, % |
|---|---|---|---|
| 399 (8.34) | 0.125 | 21.1 | 21.0 |
| 862 (18.01) | 0.146 | 26.6 | 25.2 |
| 1173 (24.49) | 0.157 | 28.7 | 28.6 |
| 1011 (21.12) | 0.086 | 19.8 | 19.5 |
| 1398 (29.20) | 0.108 | 25.1 | 25.1 |
| 1705 (35.61) | 0.120 | 28.2 | 30.9 |
| 1491 (31.15) | 0.066 | 18.5 | 19.6 |
| 1918 (40.05) | 0.086 | 23.9 | 24.1 |
| 2125 (44.39) | 0.102 | 27.4 | 29.3 |

Table 1. Comparison of gas holdup measurements based on gamma-densitometry tomography (GDT) and differential pressure (DP) results.

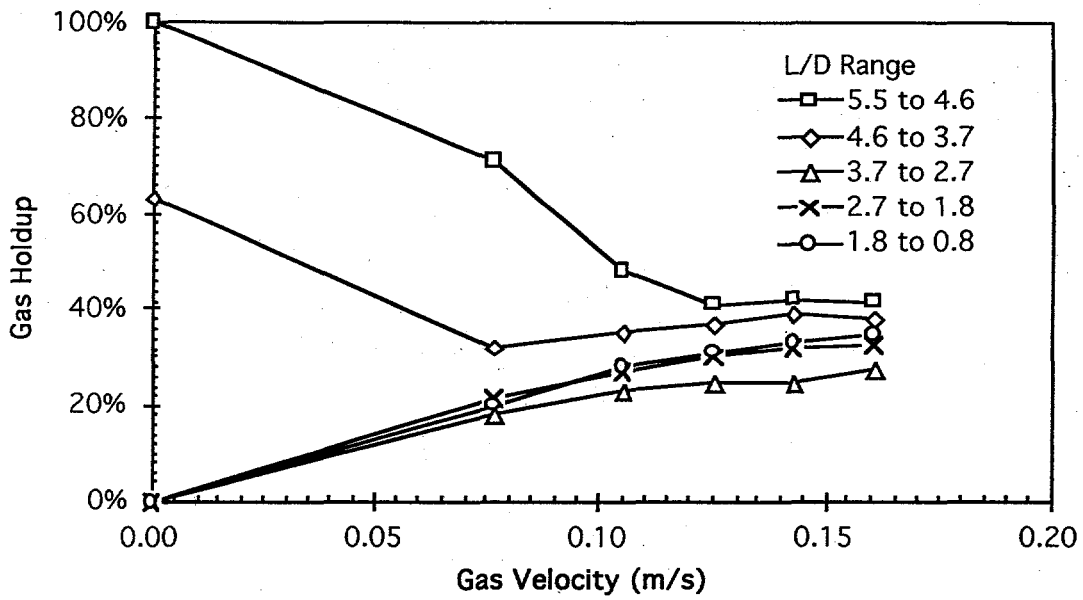


Figure 4. Axial variation (L/D range) in gas holdup (gas volume fraction) versus superficial gas velocity as determined from pressure measurements. The system pressure was 165 kPa for this test.

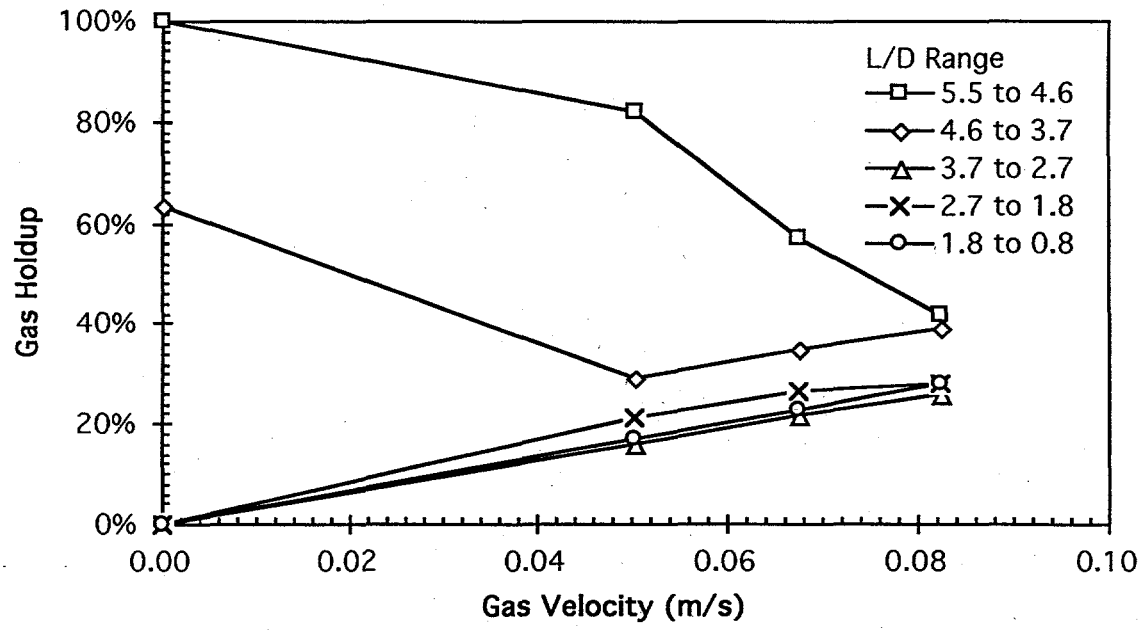


Figure 5. Axial variation (L/D range) in gas holdup (gas volume fraction) versus superficial gas velocity as determined from pressure measurements. The system pressure was 345 kPa for this test.

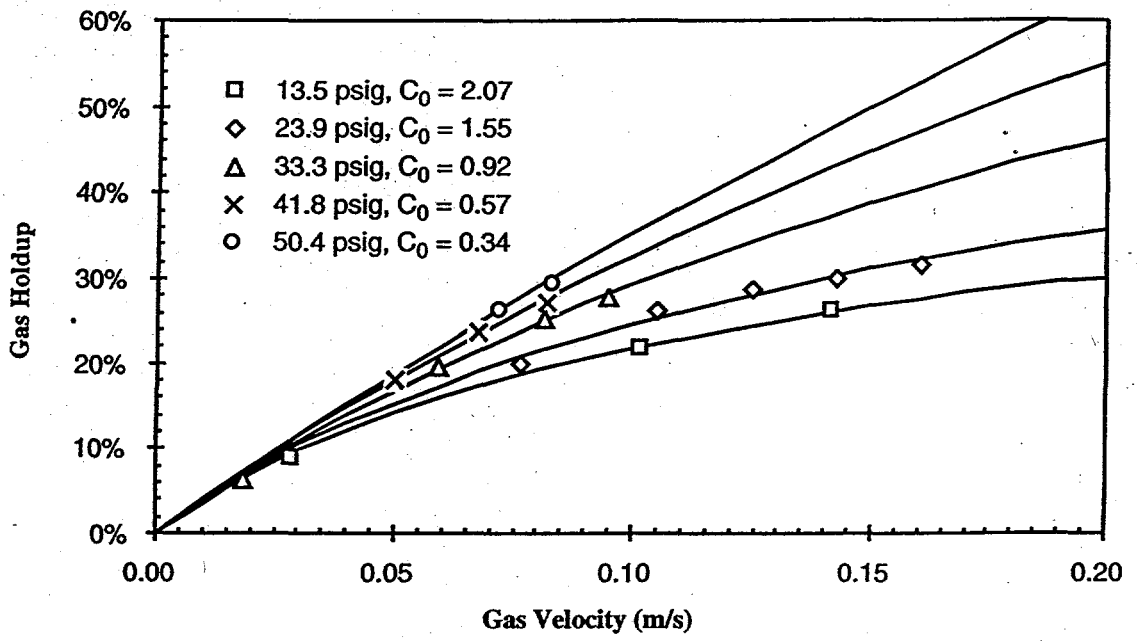


Figure 6. Gas holdup as a function of superficial gas velocity for operating pressures from 93 kPa (13.5 psig) to 347 kPa (50.4 psig). Symbols are experimental data and lines are Zuber and Findlay (1965 ) correlation.

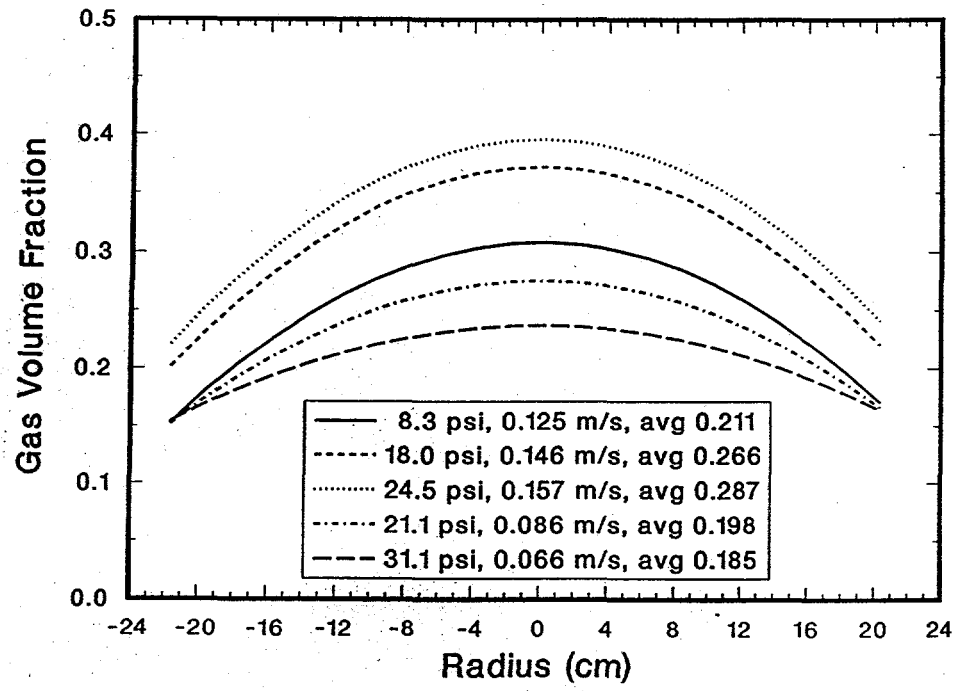


Figure 7. Radial distribution of the gas holdup for several cases as measured with gamma tomography.

## CONCLUSIONS

Differential pressure (DP) and gamma-densitometry tomography (GDT) measurements were made to determine the gas distribution in a two-phase, industrial scale, bubble column. GDT results provided measurements of the time-averaged cross-sectional distribution of gas in the liquid, and the DP measurements gave the time and volume averaged axial distribution of gas. The results showed close agreement between the two methods of measuring the gas distribution in the bubble column. GDT results showed the gas holdup was higher near the center of the column, but the distribution became flatter as the superficial gas velocity decreased. DP results showed that the gas holdup was nearly uniform along the length of the column, except in the region about one diameter from the surface. The results also were able to detect the increase of gas volume fraction in the liquid that corresponds to an increase in system pressure at a fixed volumetric flowrate. Further tests will be performed in the future to determine the independent impact of system pressure and superficial gas velocity.

## ACKNOWLEDGMENTS

The authors would like to express their thanks to Tom Grasser, John O'Hare, and C. "Buddy" Lafferty for the assistance they provided in getting the bubble column and GDT system operational. We would also like to thank Ron Dykhuizen for his keen insights about two-phase flows. This work was performed at Sandia National Laboratories, supported by the U. S. Department of Energy under contract number DE-AC04-94AL85000, through a laboratory directed research and development contract.

## REFERENCES

Brown, G. O., Stone, M. L., and Gazin, J. E., 1993, "Accuracy of Gamma Ray Computerized Tomography in Porous Media," *Water Resources Reseach*, Vol. 29, No. 2, 479-486.

Cheremisinoff, N. P., and Gupta, R., ed., 1983, *Handbook of Fluids in Motion*, Ann Arbor Science Publishers, Ann Arbor, MI, pp. 592-595.

Davidson, J. F., and Schuler, B. O. G., 1960, "Bubble Formation at an Orifice in an Inviscid Liquid," *Trans. Instn. Chem. Engrs.*, Vol. 38, pp 335-342.

Herman, G. T., 1983, "The Special Issue on Computerized Tomography," Proceedings of the IEEE, Vol. 71, No. 3, pp. 291-292.

Howard, J. N., ed., 1985, *Measurement of Two-Phase Flow Parameters*, Academic Press, London.

Knoll, G. F., 1979, *Radiation Detection and Measurement*, John Wiley & Sons, New York, NY, pp. 96-99.

Kumar, S. B., Moslemian, D., and Dudukovic, M. P., 1995, "A Gamma-Ray Tomographic Scanner for Imaging Voidage Distribution in Two-Phase Flow Systems," *Flow Meas. Instrum.*, Vol. 6, No. 1, pp. 61-73.

LaNauze, R. D., and Harris, I. J., 1974, "Gas Bubble Formation at Elevated System Pressures," *Trans. Instn. Chem. Engrs.*, Vol. 52, pp 337-348.

Reda, D. C., Hadley, G. R., and Turner, J. R., 1981, "Application of Gamma-Beam Attenuation Technique to the Measurement of Liquid Attenuation for Two-Phase Flows in Porous Media," *Instrumenttation in the Aerospace Industry*, Vol. 27, Part Two, *Proceedings of the 27th International Instrumentation Symposium*, K. E. Kissell, ed., Instrument Society of America, Research Triangle Park, NC, pp. 553-568.

Torczynski, J. R., Adkins, D. R., Shollenberger, K. A., and O'Hern, T. J., 1996, "Application of Gamma-Densitometry Tomography to Determine the Phase Spatial Variation in Two-Phase and Three-Phase Bubbly Flows," Cavitation and Multiphase Flow Forum, J. Katz, ed., ASME, NY, submitted.

Zuber, N., and Findlay, J. A., 1965, "Average Volumetric Concentration in Two-Phase Flow Systems," *Journal of Heat Transfer*, Vol. 87c, pp. 453.

## DISCLAIMER

SAND96-0440C

1996 National Heat Transfer Conference
Instrumentation and Measurements Symposium
August 3-6, 1996, Houston, TX SAND96-XXXXC

# PRESSURE EFFECTS ON BUBBLE-COLUMN FLOW CHARACTERISTICS

D. R. Adkins, K. A. Shollenberger, T. J. O'Hern, and J. R. Torczynski
Engineering Sciences Center
Sandia National Laboratories
Albuquerque, NM 87185

## ABSTRACT

Bubble-column reactors are used in the chemical processing industry for two-phase and three-phase chemical reactions. Hydrodynamic effects must be considered when attempting to scale these reactors to sizes of industrial interest, and diagnostics are needed to acquire data for the validation of multiphase scaling predictions. This paper discusses the use of differential pressure (DP) and gamma-densitometry tomography (GDT) measurements to ascertain the gas distribution in a two-phase bubble column reactor. Tests were performed on an industrial scale reactor (3-m tall, 0.48-m inside diameter) using a 5-Curie cesium-137 source with a sodium-iodide scintillation detector. GDT results provide information on the time-averaged cross-sectional distribution of gas in the liquid, and DP measurements provide information on the time and volume averaged axial distribution of gas. Close agreement was observed between the two methods of measuring the gas distribution in the bubble column. The results clearly show that, for a fixed volumetric flowrate through the reactor, increasing the system pressure leads to an increase in the gas volume fraction or "gas holdup" in the liquid. It is also shown from this work that GDT can provide useful diagnostic information on industrial scale bubble-column reactors.

## NOMENCLATURE

$a_0$ = constant term of $\psi(r,R)$ curve fit (nondimensional)
$a_1$ = quadratic term of $\psi(r,R)$ curve fit (nondimensional)
$b_0$ = constant term of $\psi(x,R)$ curve fit (nondimensional)
$b_1$ = quadratic term of $\psi(x,R)$ curve fit (nondimensional)
$g$ = gravitational acceleration (m/s$^2$)
$u_g$ = superficial gas velocity (m/s)
$r$ = radial location (m)
$u_l$ = superficial liquid velocity (m/s)
$x$ = cross-section location of gamma trace (m)
$z$ = axial location (m)
$D$ = column inner diameter, $D = 2R$ (m)
$I$ = gamma intensity (photons/s)
$I_o$ = incident intensity (photons/s)